The Glycine Box: A Determinant of Specificity for Fibroblast Growth Factor†

Yongde Luo, Weiqin Lu, Khalid A. Mohamedali, Jun-Hyeog Jang, Richard B. Jones, Jerome L. Gabriel,‡ Mikio Kan, and Wallace L. McKeehan*

Center for Cancer Biology and Nutrition, Institute of Biosciences and Technology and Department of Biochemistry and Biophysics, Texas A&M University, 2121 W. Holcombe Boulevard, Houston, Texas 77030-3303

Received July 13, 1998; Revised Manuscript Received September 16, 1998

ABSTRACT: Acidic fibroblast growth factor (FGF-1), keratinocyte growth factor (FGF-7), and FGF-10 are homologues with distinct specificity. In the presence of heparin, FGF-1 binds and activates in vitro all FGFR subtypes, while FGF-7 exhibits absolute specificity for the IIIb splice variant of FGFR2. FGF-10 exhibits a similar specificity but also binds the FGFR1IIIb isoform. Neither FGF-7 nor FGF-10 will bind to IIIc isoforms of FGFR. Molecular models of FGF, heparin, and the FGFR ectodomain suggested that sequences between β-strands 10 and 12 of FGF may be important for the interaction of FGF with the heparin−FGFR ectodomain duplex. Site-directed mutants of FGF-7 and FGF-10 were prepared to test whether this domain might underlie failure of FGF-7 and FGF-10 to bind to the FGFRIIIc isoforms. Constructions with substitution of FGF-1 sequences spanning the entire C-terminus encoded in exon 3 or only C-terminal sequences spanning β-strands 10 through 12 conferred ability on FGF-7 to bind to and activate FGFRIIIc without a significant loss in binding to or activation of FGFR2IIIb. A series of twelve different substitutions of shorter segments of FGF-1 sequences into the C-terminal portion of FGF-7 or FGF-10 revealed that substitution of GSCKRG for GIPVRG or the tri-peptide sequence KKN for NQK just N-terminal to it conferred dual activities on both the FGF-7 and FGF-10 backbones. The results suggest that the combined sequence domain, which we call the FGF glycine box (G-box), is a major determinant for the specificity of the binding of FGF to heparan sulfate−FGFR duplexes.

The fibroblast growth factor (FGF[1]) signal transduction system is a tripartite complex, a ubiquitous, and an intrinsic mediator of embryonic development and adult tissue homeostasis (*1*). The family is currently comprised of seventeen FGF polypeptides, an extensive array of alternately spliced products of four transmembrane tyrosine kinase receptor genes, and less well-characterized heparan sulfates from the peri-cellular matrix that are mimicked experimentally by heparin. Structural homologues of the FGF family are characterized by homologous sequence domains encoded by three exons whose structure has been resolved for FGF-1 (*2*) and FGF-2 (*2*−*5*) by X-ray crystallography. When analyzed in vitro with heparin as cofactor, FGFs exhibit both cross-reactivity and specificity for isotypes of the FGFR kinase ectodomain (*1, 6*). FGF-1 is the least specific and acts in vitro on all isoforms of FGFR examined to date. In contrast, FGF-7 (also called keratinocyte growth factor or KGF), whose expression is limited to stromal or mesenchymal cells in tissues with both mesenchymal and epithelial compartments, is the most specific and acts only on epithelial cell FGFR2IIIb (*1, 6*−*8*). FGF-3, whose expression is restricted during development and to some tumors (*9*), also acts on FGFR2IIIb as well as FGF-10, whose expression is also limited to specific stromal or mesenchymal cells in development and the adult (ref *10* and Lu, Luo, Kan, and McKeehan, manuscript in preparation). In contrast to FGF-7, FGF-3 (*6*) and FGF-10 (Lu, Luo, Kan, and McKeehan, manuscript in preparation) also bind to FGFR1IIIb.

From the crystal structures of FGF-1 and FGF-2 and cassette mutagenesis, the notable solvent-exposed loop comprised of unique sequences among FGFs between β-strands 9 and 10 has been proposed to potentially underlie the rejection of FGF-7 by the IIIc isoforms of FGFR (*11, 12*). Sequence swapping experiments between large segments of FGF-7 and FGF-2 suggested that the N-terminal part of FGF-7 and FGF-2 determined respective specificity for FGFR (*13*). More recently, it has been demonstrated that the homologue of FGF-3 from Xenopus binds both FGFR2IIIb and IIIc variants in contrast to mouse and zebrafish FGF-3, which bind specifically FGFR2IIIb (*9*). Replacement of the C-terminal sequence of zebrafish FGF-3 with that from Xenopus conferred the ability to stimulate cells expressing FGFR2IIIc with only a small loss in activity for FGFR2IIIb (*9*). Peptide inhibition experiments also

†This work was supported by Public Health Service Grant Nos. DK40739 and DK35310 from the National Institute of Diabetes and Digestive and Kidney Diseases and CA59971 from the National Cancer Institute (to W.L.M.).

* To whom correspondence should be addressed: Albert B. Alkek Institute of Biosciences and Technology, Department of Biochemistry and Biophysics, Texas A&M University, 2121 W. Holcombe Blvd., Houston, TX 77030-3303. Tel. 713-677-7522. Fax: 713-677-7512. E-mail: wlmckeehan@ibt03.tamu.edu.

‡ Present address: Department of Biochemistry, Temple University School of Medicine, 3420 N. Broad St., Philadelphia, PA 19140.

[1] Abbreviations: FGF, fibroblast growth factor; FGFR, FGF receptor kinase; FGFR1−4, type 1 through 4 of the FGFR kinases; KGF, keratinocyte growth factor, acronym for FGF-7; G-box, FGF glycine box; GST, glutathione-S-transferase; IPTG, isopropyl-1-thio-β-D-galactopyranoside; GSH, glutathione; PBS, phosphate buffered saline; SDS−PAGE, sodium dodecyl sulfate−polyacrylamide gel electrophoresis; PCR, polymerase chain reaction; MK, mouse keratinocytes; NIH 3T3, fibroblast-like mesenchymal cells; IL1β, interleukin-1 β.

10.1021/bi9816599 CCC: $15.00
Published on Web 11/04/1998

indicate that specific epitopes within the C-terminus downstream of β-strand 9 may be important in the binding of FGF to FGFR (*14*−*16*).

In previous reports, we have shown that the rejection of FGF-7 by the IIIc isoforms of FGFR1 and FGFR2 occurs by a negative reaction with invariant sequence domains within the N-terminal half of immunoglobulin (Ig) module III, which is indirectly modified by the presence of the IIIb sequence in the C-terminal half to permit FGF-7 binding (*11*). In absence of C-terminal sequences past β-strand B in Ig module III, a duplex of the remaining fragment as short as Ig module II alone and heparin binds FGF-1, FGF-2, and FGF-7 (*11, 17*). In this report, we show that substitution of the coding sequence spanning exon 3 from the end of β-strand 7 through 12 at the C-terminus of FGF-7 with that of FGF-1 conferred ability to bind and activate FGFR2IIIc with an efficiency only three times less than for FGFR2IIIb. Replacement of the inter-β-strand 10/12 sequence of FGF-7 with the FGF-1 sequence yielded an FGF with equal activity for both FGFR2 variants. Replacement of the sequence GIPVRG which was assigned β-strand 11 from a secondary structure analysis, but is an α-helix in solution in FGF-2 (*18*) with the homologous FGF-1 sequence or the tri-peptide sequence N-terminal (NQK to KKN) to it, also conferred activity for FGFR2IIIc on FGF-7 with retention of activity for FGFR2IIIb. Cassette substitution or mutations of the solvent-exposed loop sequence that bridges β-strands 9 and 10, β-strand 10, or sequences between β-strand 11 and 12 had no effect on the specificity of FGF-7 for FGFR2IIIb. These results suggest that the sequence NQKGIPVRG in FGF-7, which we refer to as the "glycine or G-box", is a major determinant of specificity for the heparan sulfate−FGFR kinase duplex.

MATERIALS AND METHODS

Production and Recovery of Recombinant FGF. Expression, recovery, and purification of recombinant FGF-1, FGF-7, FGF-10, and mutant constructions were carried out by a novel combination of bacterial expression and recovery methods. Each FGF was expressed as a fusion protein with bacterial glutathione-S-transferase (GST) at the N-terminus. GST was fused at Ala-30, Ala-69, and Ala-1 of FGF-7, FGF-10, and FGF-1, respectively. *Escherichia coli* BL21 (DE3) were transformed and incubated overnight at 37 °C in LB medium containing ampicillin (50 μg/mL) until cell density reached an OD_{600} of 0.6−1.5. The cells were then transferred to 30 °C, and 0.4 M isopropyl-1-thio-β-D-galactopyranoside (IPTG) was added to the medium to induce expression of the recombinant product. After incubation for 3−4 h, the bacteria were collected by centrifugation and the resulting pellet was frozen at −80 °C. The cell pellet was then resuspended in 25 mM Tris-HCl (pH 7.2), 1 mM EDTA, 0.6−0.9 M NaCl, and 1 mM phenylmethylsulfonyl fluoride (PMSF), and then the cells were lysed by sonication and clarified by centrifugation. Densities of bacteria transformed with cDNAs coding for FGF-7 and mutant constructs were brought to maximum, usually OD_{600} of 1.2−1.5 prior to induction by IPTG. Under these improved conditions, the yields of FGF-7 and its mutants were 20−33% of those of FGF-1 and FGF-10 compared to yields that were 5% or less at densities of 0.6−1.0.

Soluble recombinant product was recovered from bacterial lysates by a combination of chromatography on GSH−agarose and heparin−agarose. After application of supernatant containing the recombinant GST−FGF fusion product to the GSH−agarose column, the beads were washed with phosphate buffered saline (PBS) until the absorbance fell to baseline, and then the column was eluted with 10 mM glutathione (GSH) in 25 mM Tris-HCI (pH 7.0) and 1 mM EDTA. The eluate was then applied to a heparin−agarose column (1 mL of sample/0.5 mL slurry of beads). After an extensive wash with PBS, the GST and a portion of the N-terminal sequence was removed by incubation of the immobilized fusion product with 2−5 μg/mL trypsin in PBS for 40 min at room temperature. Following the incubation, the column was extensively washed with PBS containing the maximum NaCl (0.6−0.9 M) possible, which did not elute the particular FGF construct. The product was then eluted with 2 M NaCl in PBS and further purified by FPLC using a heparin−agarose column. Purity and the amount of factors were determined by 15% SDS−polyacrylamide gel electrophoresis and absorbance at 280 nm.

Construction of Models of the FGF−Receptor Complex. Atomic models of the FGFR complex were modified from those previously described using the same methods (*19*). Since a structure of FGF-7 is unavailable, a model of FGF-7 and a ternary complex of FGF-7, heparin, and the FGFR ectodomain using residues 66−194 of FGF-7 was created as follows: Homologous β-strand sequences in FGF-7 and FGF-1 in the previously described ternary complex (*19*) were aligned, followed by the insertion of interstrand loop residues specific for FGF-7. Molecular dynamics calculations (200 ps) were performed on the FGF-7 complex as described (*19*). A ternary complex (not shown) of FGF-1, hexadecameric heparin, and FGFR2IIIb was built by the same approach described for the published FGF-1−heparin−FGFR1IIIc complex (*19*). An initial model of the ternary complex was constructed by first overlaying onto and then substituting the model of FGF-7 with the FGF-1 part of our original ternary complex. The model was refined using molecular dynamics calculations followed by energy minimization as described for the FGFR1IIIc complex (*19*). To study the basis for rejection of FGF-7 from FGFR1IIIc, FGF-7 was overlaid on FGF-1 that was part of the FGF-1−heparin−FGFR1IIIc complex and the interactions between them were studied in detail. As a control, FGF-2 was also superimposed in this manner and its interactions with the FGFR1IIIc−heparin duplex were examined. Models of ternary complexes of mutants of the FGF-7 backbone were constructed by substitution of the mutant sequence into FGF-7 within the ternary complex followed by molecular dynamics calculations and energy minimization.

Construction of Mutant FGF cDNAs. Oligonucleotides employed in construction of recombinant FGF constructions were purchased from Integrated DNA Technologies, Inc. (Coralville, IA) and are listed below. Restriction sites are underlined, and nucleotides not in the coding sequence for FGF are in lowercase. Sequences from FGF-1 are italicized. FGF-7: K1, cgggatccGCTTGCAATGACATGAGT; K2, gggaattcTTAAGTTATTGCCATAGG; K3, GGGGAGCTC-TATGCAAAG*CAGACACCAAATGAGGAA*; K4, CTTTG-CATAGAGCTCCCC; K5, *ATATCCAAGAAGCATGCA-GAGAAGAATTGG*TTCGTGGCCTTAAATCAAAAG; K6,

C C A A T T C T T C T C T G C A T G C T T C T T G G A T A-*T*ATAGGTGTTGTAATGGTTTTC; K7, GAAATGTTCGTG-GCCTTA*AAGAAGAATGGGAGCTGC*; K8, *CTTCTT*TAAG-GCCACGAACATTTC; K9, TTAAGTTATTGCCATAGGAAGAAA-*CAAGATTGCTTTCTG*; K10, *CCTCGGACTCACTATGGC*-CAAAAAACGGCCCACTTT; K11, TTG*GCCATAGT-GAGTCCGAGG*CCCTTTGACAGGAAGCCC; K12, GGG-*GCAGCCACGAAGGCCGAA*CAAAAAACGGCCCAC; K13, *TTCGGCCTTCGTGGCTGC*CCCTTTGACAG-GAAGCCCCTT; K14, *CCTCGGACTCACTATGGC*; K15, *GCCATAGTGAGTCCGAGG*; K16, *AATGGGAGCTGCAAAC-GC*GGGAAGAAAACGAAGAAA; K17, *GCGTTTG-CAGCTCCCATTCTTCTT*TAAGGCCACGAACATTTC; K18, *GGGAGCTGCAAACGC*GGGAAGAAAACGAA-GAAA; K19, CCC-*GCGTTTGCAGCTCCC*CTTTTGATT-TAAGGC; K20, TTA*AAGAAGAAT*GGGCTTCCTGTCAAA; K21, AAGCCC*ATTCTTCTT*TAAGGCCACGAACATTTC; K22, GGGGAA*TGGTTCGTGGG*CTTA; K23, G*CCCAC-GAACCA*TTCCCCTCC. FGF-10: T1, gcggatccGCGGG-GAGGCATGTGCGA; T2, gggaattcCTATGAGTGGAC-CACCAT; T3, CAAATGTACGTGGCCTTG*AAGAAGAA-TGGGAGCTGC*; T4, CAAGGCCACGTACATTTG; T5, *G G G A G C T G C A A A C G C G G T*C A A A A A A C A A-GAAGGAAA; T6, *ACCGCGTTTGCAGCTCCC*TTTTC-CATTCAATGCCAC. FGF-1: A1, ggggatcc*ATGGCT-GAAGGGGAAATC*; A2, gcgaattc*TTAATCAGAAGAGACTGG*.

Rat FGF-7 (residues 30−194), rat FGF-10 (residues 69−215), and human FGF-1 (residues 1−154) cDNAs were used as templates in the polymerase chain reaction (PCR) to generate cDNAs coding for the constructions summarized in Figure 5. Primer pairs K1 and K2 and T1 and T2 were used to amplify the coding sequences of FGF-7 and FGF-10 constructs, respectively. Most of the substitution mutants were constructed by the overlapping extension strategy. 7m1 was generated by a second PCR using primer pairs K1 and A2 and the two first-round PCR products as templates by amplifying FGF-1 with primers K3 and A2 and amplifying FGF-7 with primers K4 and K1. 7m2 was constructed by a second PCR using primer pairs K1 and K2 and two PCR products as templates by amplifying FGF-7 with primer pairs K5 and K2 and K6 and K1, respectively. The same procedure used for 7m2 was utilized for the following constructs: 7m4 with primers K7, K9, and FGF-1 template and K8, K1, and FGF-7 template; 7m5 with primers K10, K2, K11, K1, and FGF-7 template; 7m6 with primers K12, K2, K13, K1, and FGF-7 template; 7m7 with primers K14, K2, and 7m5 template and K15, K1, and 7m4 template; 7m8 by primers K10 and K2 and 7m4 template, and K11 and K1, and FGF-7 template; 7m9 by primers K16, K2, K17, K1, and FGF-7 template; 7m10 by primers K18, K2, K19, K1, and FGF-7 template; 7m11 by primers K20, K2, K21, K1, and FGF-7 template; 7m12 by primers K22, K2, K23, K1 and FGF-7 template. Mutant 10m1 was generated by a second PCR using primer pairs T1 and A2 and two first-round PCR products by amplifying FGF-1 with primers T3 and A2 and amplifying FGF-10 with primers T4 and T1. 10m2 was constructed in a second PCR using primer pairs T1 and T2 and two PCR products by amplifying FGF-10 with primer pairs T5 and T2 and T6 and T1, respectively. 7m3 was created by ligation of the 376-bp fragment from 7m2 and 120 bp from FGF-1 after *Sph*1 restriction enzyme digestion.

All PCRs were performed for 30 cycles at 96 °C for 1 min, 60 °C for 1 min 20 s, and 72 °C for 1 min. The second-step PCR products were digested by *Bam*H1 and *Eco*R1, purified by electroelution, and cloned into the pGEX-2T vector at *Bam*H1 and *Eco*R1 sites. Each construct was used to transform expression host BL21 (DE3) cells (Novagen, Madison, WI), and colonies were selected on ampicillin-containing LB plates. The sequence of each mutant construct was confirmed in pGEX-2T directly with the Sequence Quick-Denature Plasmid Sequencing Kit (U.S. Biochemical Corp.)

Competition Binding Assays. Native bovine FGF-1 was purified from bovine brains, iodinated, and employed as a radiolabeled standard FGF which binds equally in the presence of heparin to all forms of recombinant FGFR and cell types employed in the study. Covalent affinity cross-linking and the binding of ^{125}I-FGF-1 to specific FGFR kinase sites was distinguished from nonspecific binding and binding to pericellular heparan sulfate sites as described (*20, 21*). FGFR isoforms were expressed on the surface of baculoviral-infected Sf9 insect cells under optimized conditions as described (*11*).

Mitogenic Activity. DNA synthesis was measured by incorporation of [^{3}H]-thymidine into subconfluent mouse keratinocytes (MK) and mouse 3T3 fibroblasts in the presence of 10 μg/mL heparin as described (*19, 20*). These two models were chosen because of their common robust response to FGF-1 and differential response to FGF-7 under a range of culture conditions, which has been documented by both our laboratory (*19, 20*) and others (*13, 22*−*24*). Mitogenic activity was expressed as the mean percentage of maximum thymidine incorporation promoted by FGF-1 in 3T3 cells and FGF-7 in MK cells. Variation among replicate assays within a single experiment was less than 10%.

RESULTS

Expression and Recovery of Recombinant FGF-7, FGF-10, and Mutant Constructs from Bacteria. Despite improvement by expression of less than full-length cDNAs (*22*), yields of recombinant FGF-7 from bacteria were sufficiently low relative to FGF-1 and FGF-2 to hamper construction and routine analysis of a wide spectrum of mutants using the FGF-7 backbone structure. In addition, FGF-7 elutes at significantly lower concentrations of salt from heparin−agarose than from FGF-1 and FGF-2. This decreased the utility of the heparin affinity purification procedure for removal of contaminating proteins that elute prior to FGF. To improve expression and recovery of FGF-7 and mutants from bacteria, we developed a new procedure (Materials and Methods) which may apply to expression and recovery of all members of the FGF family. The process employed both the expression of an inactive fusion protein and subsequent release and activation of the FGF-7 portion by proteolytic processing at a natural cleavage site in the N-terminus of FGF-7. The process exploited previous findings with FGF-1 that demonstrated that heparin protects the active core of FGF from proteolysis (*19*). FGF-7 beginning at Ala-30 was expressed as an inactive 45-kDa fusion product with GST at its N-terminus (Figures 1, 2). The GST portion was exploited for recovery of the product containing only intact fusion protein by GSH affinity chromatography. The inac-

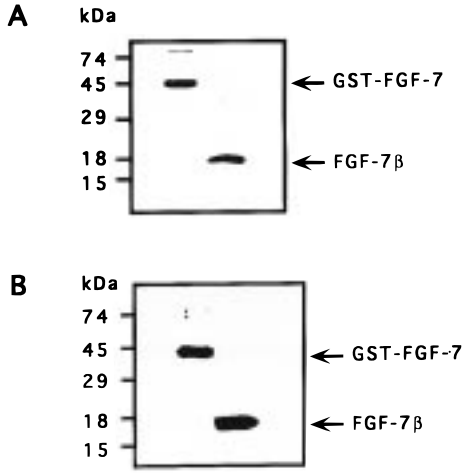

FIGURE 1: Generation and analysis of FGF-7 from heparin-immobilized GST−FGF-7 by trypsin. GST−FGF-7 fusion product was purified from bacterial lysates by GSH−agarose chromatography, applied to heparin−agarose, treated with trypsin, and analyzed by SDS−PAGE as described in Materials and Methods. The left lane and right lane are the eluates from GSH−agarose and heparin−agarose, respectively. Panel A was visualized by silver stain and panel B by immunoblot with rabbit anti-serum prepared against purified FGF-7β (^{54}Ser-FGF-7). In separate experiments, the right lane was excised and subjected to N-terminal microsequencing.

tive GST−FGF-7 fusion product retained affinity for heparin. Treatment of heparin-immobilized GST−FGF-7 with trypsin resulted in removal of the GST portion with retention of an active 17 kDa FGF-7 core that was protected from further digestion (Figure 1). The FGF-7 core remained bound to the heparin−agarose while trypsin, trypsin inhibitors, and minor contaminants were removed by washing with PS containing 0.6 M NaCl. Trypsin treatment of the immobilized FGF-7 also had the added benefit of destroying other proteins that are not specifically protected by heparin. Amino-terminal sequencing revealed that the process yielded an FGF-7 beginning with Ser-54, indicating that trypsin cleaved the N-terminal part of the fusion product at Arg-53. ^{54}Ser-FGF-7 has been shown by sequential deletion mutagenesis to be the shortest form of bacterial FGF-7 that retains full activity in vitro, and proteolytic modification occurs at the site in mammalian cells (*23, 24*). The combined process improved both the number of total mutants that could be expressed and recovered in quantities sufficient for analysis and yields of all constructs based on FGF-7. The procedure was subsequently applied to FGF-1 and FGF-10 with significant improvement in yields of pure full-length products. Sequence analysis revealed that the process yielded ^{15}Phe-FGF-1 and ^{75}Ser-FGF-10, which are residues that are spatially homologous to Ser-54 in FGF-7. Results to be reported elsewhere indicate that this procedure applies to other members of the FGF family and reflects a natural process of modification of the N-terminus of heparan sulfate-bound FGF by cell surface proteases.

Prediction of the Basis for Rejection of FGF-7 by FGFR1IIIc by Molecular Modeling. In lieu of direct structural data on the FGFR ectodomain, we have employed atomic models of a ternary complex of the FGFR ectodomain, heparin, and the resolved structures of FGF-1 and FGF-2 which accommodate the most available data to guide experimental tests of structure−function analysis of the three

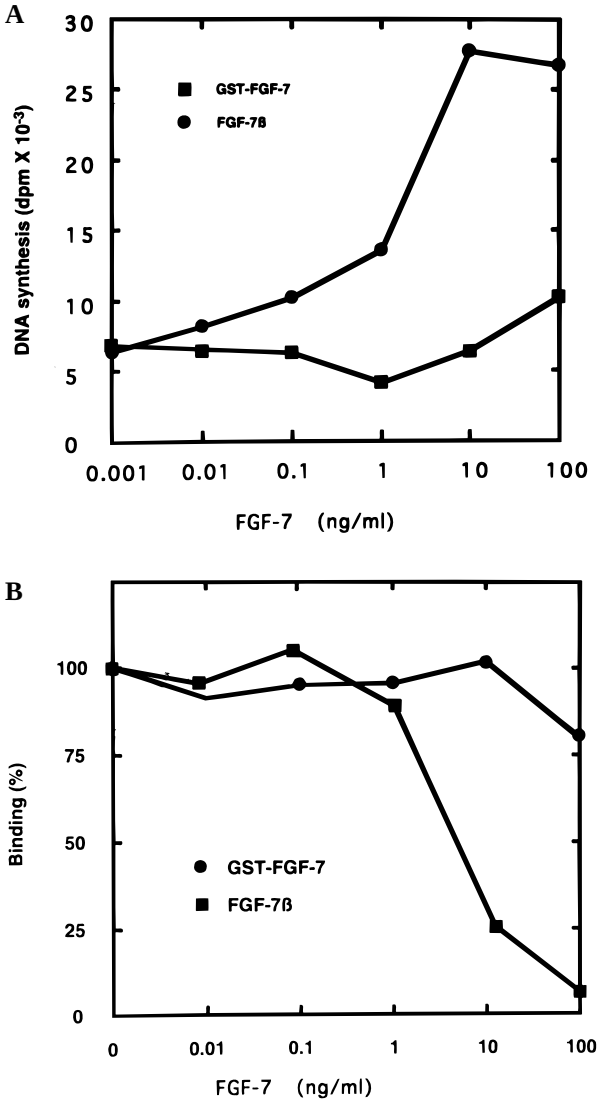

FIGURE 2: Activity of GST−FGF-7 and derived FGF-7. GST−FGF-7 from the GSH−agarose column and FGF-7β (^{54}Ser-FGF-7) from the heparin−agarose column described in Figure 1 prior to further purification by FPLC were tested at the indicated concentrations in MK keratinocyte cell growth assays (panel A) or for competition with radiolabeled FGF-1 binding to FGFR2IIIb expressed on the surface of baculoviral-infected insect cells (panel B) by procedures described in Methods.

components (*11, 19, 25*). A model of sequence residues 66−194 of FGF-7, whose crystal structure has not yet been resolved, was superimposed on the template of bovine FGF-1 in our previously published (*19*) ternary complex with heparin and FGFR1IIIc (Figure 3A). The model was examined in detail for conflicting interactions between residues of the three components. Most notable was the proximity and intertwining of specific residues from β-strand 11, assigned from crystal structures of FGF-1 and FGF-2, with the fl1-C strand junction of Ig module III of FGFR1IIIc (Figure 3A). In addition, we noted a potential charge conflict between the lysine-rich portion (KKTKK) of the inter-β-strand 11/12 sequence of FGF-7 with the lysine residue of the unique KE insertion in the E strand of exon IIIc. Neither of the two areas of conflict was observed in a model of FGF-7, heparin, and FGFR2IIIb (Figure 3B). Moreover, the potential conflicts were not apparent in model ternary complexes comprised of FGF-7 in which the C-terminus was

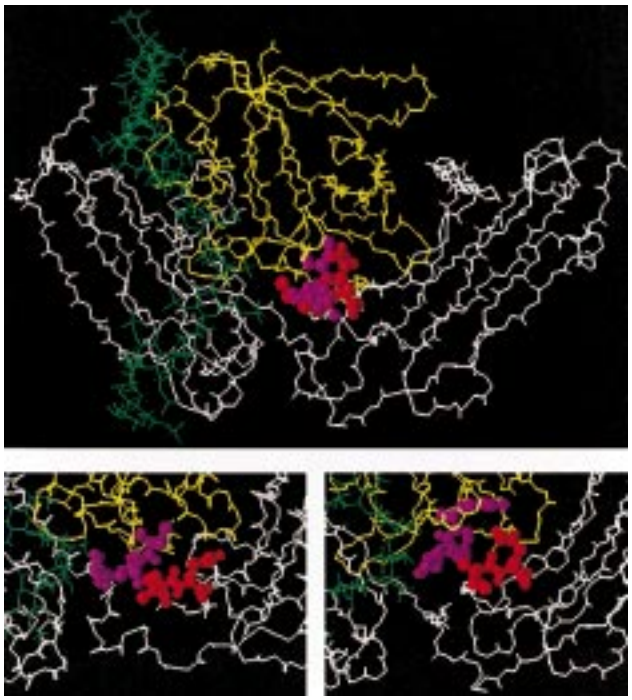

FIGURE 3: Molecular models of wild-type FGF-7 and an FGF-7−FGF-1 (7m4) chimera docked into duplexes of heparin and FGFR1IIIc or FGFR2IIIb ectodomains. Models of ternary complexes of the indicated FGF, FGFR, and hexadecameric heparins were constructed as described in Materials and Methods. Receptor ectodomains are in white, FGF in yellow, and heparin in green. Appropriate ligand and receptor residues are highlighted to show the spatial conflict that exists between these residues when FGF-7 is docked into the FGFR1IIIc−heparin duplex (top panel) and the absence of the conflict in the FGF-7−FGFR2IIIb−heparin complex (bottom left). The conflict is also eliminated in the complex of heparin−FGFR2IIIc and the FGF-7−FGF-1 chimera 7m4 (right panel). Ligand residues are in purple (Val-173, Arg-174, and Gly-175 in FGF-7; Lys-173, Arg-174, and Gly-175 in the FGF-7−FGF-1 chimera 7m4), while Ile-198 and Gln-199 of the receptor are illustrated in red. (top panel) FGF-7 docked into a duplex of heparin and FGFR1IIIc. (bottom left panel) FGF-7 docked into a duplex of heparin and FGFR2IIIb. (bottom right panel) FGF-7−FGF-1 chimera (7m4) docked into a duplex of heparin and FGFR1IIIc.

replaced with the corresponding sequences from human FGF-1 (Figure 3C).

Substitution of C-terminal Sequences of FGF-7 and FGF-10 with Sequences from FGF-1. Since the species-specific differences in binding to FGFR2IIIb were in the C-terminal portion of FGF-3 (*9*) and our models predicted conflicts in the C-terminal portion of FGF-7 with FGFRIIIc, a series of mutant constructions with alterations or substitutions of FGF-1 sequences into the C-terminal portion of FGF-7 (mutants 7m1 to 7m12) and FGF-10 (10m1 and 10m2) were constructed (Figures 4, 5). Mutant 7m1 was constructed by substitution of the entire exon 3 of FGF-7 beginning at Lys-130 in FGF-7 with the corresponding exon 3 from FGF-1 beginning at Gln-91. Mutants 7m2 to 7m5 were constructed by substitution of specific sequence domains based on the β-strand assignments from crystal structures of FGF-1 and FGF-2. Construct 7m2 consisted of substitution of the sequence Ala-151 to Met-162 between β-strands 9 and 10, in 7m3 the entire C-terminus was substituted after β-strand 9 (Ala-151), in 7m4 the sequence between β-strands 10 and 12 (Gln-167 to His-186) was substituted, and in 7m5 the sequence between β-strand 11 and 12 (Lys-176 to Glu-181) was substituted. Construct 7m6 consisted of alteration of the FGF-7 interstrand 11/12 sequence, KKTKKE, to the sequence AATKAE since molecular modeling indicated a potential charge conflict with FGFRIIIc in that sequence (Figure 5).

Table 1: Yield, Competitive Binding, and Mitogenic Activity of Recombinant FGF Homologues[a]

	yield (percent)	binding (ng/mL)		DNA synthesis (ng/mL)	
		MK	3T3	MK	3T3
FGF-1	1000	3	3	0.05	0.9
FGF-7	100	4		0.05	
FGF-10	500	4		0.1	
7m1	300	75	240	0.8	90
7m2	2	70		9	
7m3		na	na	na	na
7m4	0.1	35	28	1.2	6
7m5	100	5		0.07	
7m6	100	4.5		0.06	
7m7		na	na	na	na
7m8	10	80		1.1	
7m9		na	na	na	na
7m10	100	6	660	0.06	300
7m11	100	4	280	0.06	70
7m12	100	6		0.08	
10m1	500	10	1600	0.4	7.5
10m2	500	6	6000	0.25	850

[a] Yields are the homogeneous products expressed and recovered by the method described in Materials and Methods. The data are expressed as the percent of the yield of FGF-7. Binding is a summary of data from Figure 7 indicating the amount of factor in nanograms per milliliters required to reduce the binding of radiolabeled FGF-1 to 50%. Mitogenic activity is a summary of the data in Figure 6 and is expressed as the amount of factor required to support a half-maximum level of DNA synthesis in the indicated cell types: na = not assayed; blank = undetectable.

On the basis of preliminary activity results and those emergent in the literature, we made six additional constructs, 7m7 through 7m12, bearing substitutions of FGF-1 sequence segments including β-strand 10, but before β-strand 12 (Figure 4). 7m10 was comprised of a substitution of β-strand 11, 7m11 consisted of substitution of the tripeptide NH_2-terminal to β-strand 11, and 7m12 consisted of substitution of only β-strand 10. In addition, constructions 10m1 and 10m2 were prepared using the FGF-10 backbone with FGF-1 substitutions between β-strand 10 and 12, and β-strand 11, respectively.

Wild-type and mutant constructions were produced, recovered, and quality-controlled by the novel procedure described above. Recovery and stability of purified soluble material was expressed relative to wild-type FGF-7 as 100%. Yields of wild-type FGF-7 and FGF-10 were about 10% and 50% of that of FGF-1, respectively (Table 1). Recovery of mutant constructs of FGF-7, 7m3, 7m7, and 7m9 was too low for quantitative functional analysis. Yields of 7m2, 7m4, and 7m8 were low but could be scaled up to levels adequate for comparative analysis (Table 1). Recovery and stability of all other mutations were equal to or exceeded that of the wild-type. Mutants exhibiting sufficient solubility, stability, and purity were then evaluated for promotion of mitogenesis of mammalian cells with different FGFR phenotypes, binding to the mammalian cells, binding to heparin, and then binding to specific recombinant FGFR expressed in insect cells.

Effect of Alterations in the C-terminus of FGF-7 and FGF-10 on Mitogenic Activity. FGF-7 and FGF-10 specifically

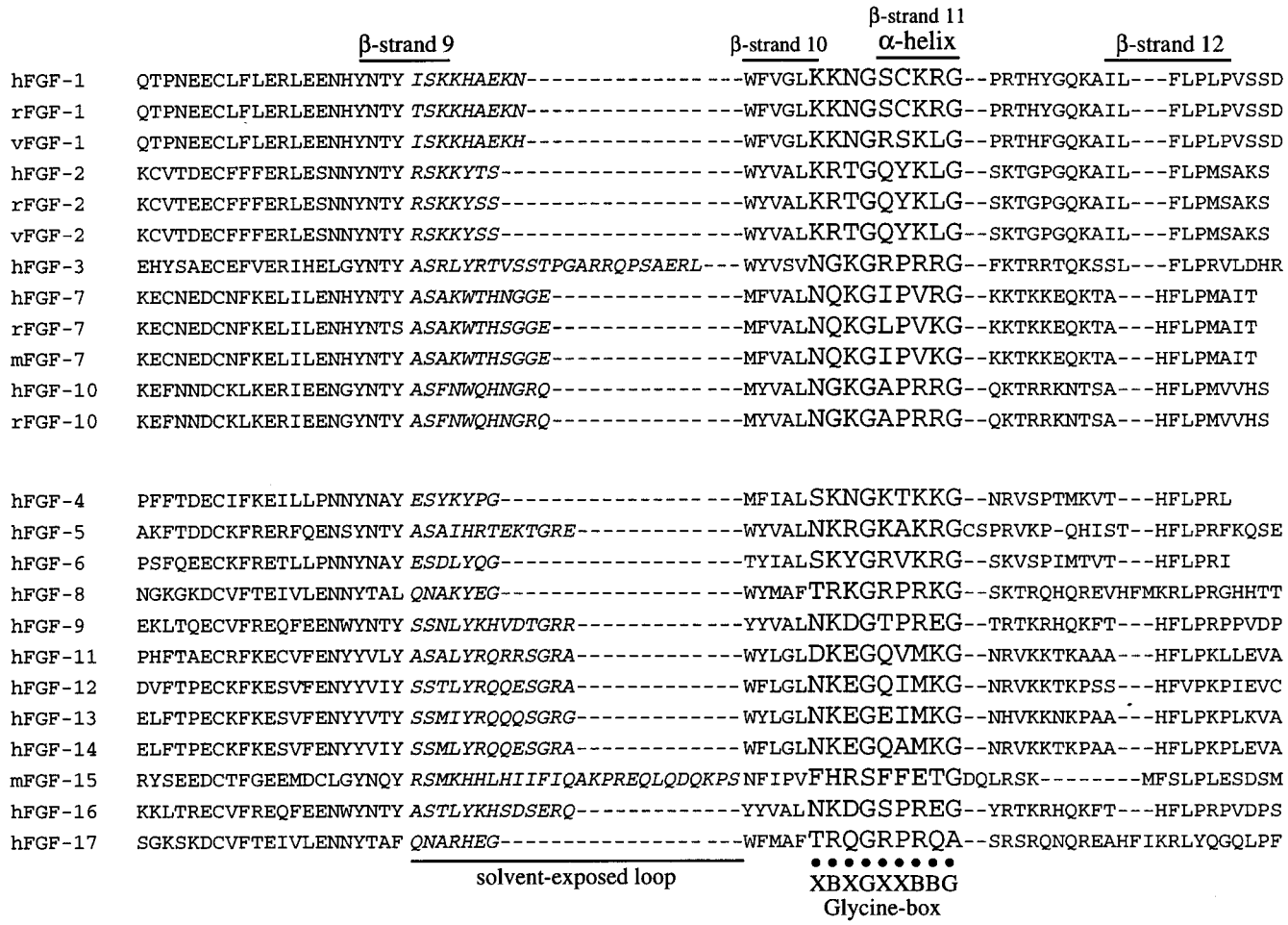

FIGURE 4: Sequence of the C-terminus of FGF encoded in exon 3. All sequences were obtained from GenBank and are from human except FGF-15, which is from mouse. Sequences for FGF-1, 2, 3, 7, and 10 begin at Gln-91, Lys-94, Glu-108, Lys-130, and Lys-150, respectively. β-strand assignments according to Zhu et al. (*2*) for FGF-2, the solvent-exposed loop (italics), and the α-helical domain in FGF-2 (*18*) are indicated. The G-box described in this report and consensus residues are indicated (X = any residue, B = basic residue, *h* = human, r = rat, v = bovine, m = mouse).

stimulate DNA synthesis of mouse keratinocyte epithelial cells (MK) which express FGFR2IIIb but fail at any concentration to stimulate fibroblast-like mesenchymal cells (NIH 3T3) which express FGFR1IIIc (Figure 6). Therefore, we first screened the panel of constructions with alterations in FGF-7 or FGF-10 for gain of activity for 3T3 cells. Constructions 7m1, 7m4, 7m10, 7m11, 10m1, and 10m2 exhibited a significant stimulation of 3T3 cell DNA synthesis (Figure 6). All mutants showing a gain of function supported a peak level of DNA synthesis of at least 85% of that supported by FGF-1. Mutants of FGF-7 (7m4) or FGF-10 (10m1) that bore the C-terminus from FGF-1 after β-strand 10 exhibited the largest gain of activity. 7m4 and 10m1 promoted a half-maximal level of DNA synthesis in 3T3 cells at 6 and 7.5 ng/mL, respectively. Next in degree of gain of function for 3T3 cells was mutant 7m1 whose substitution spanned the entire C-terminus encoded by exon 3. The potential sequences in the C-terminus underlying the gain of function were narrowed to the β-strand 11 sequence of FGF-1 (GIPVRG in FGF-7; GAPRRG in FGF-10) and the tripeptide sequence NQK which is just N-terminal to it. Mutants 7m10, 7m11, and 10m2 bearing the FGF-1 substitutions each resulted in a significant gain of activity for 3T3 cells (Figure 6). Five other constructs with changes in sequences upstream or downstream of the two short sequence domains which in combination we refer to as the "glycine or G-box" exhibited no gain of activity for 3T3 cells. The quantitative results are summarized in Table 1.

The activity of the mutant constructs 7m1, 7m4, 7m10, 7m11, 10m1, and 10m2 which exhibited a gain in activity for 3T3 cells was then compared to FGF-1 and FGF-7 for stimulation of DNA synthesis in MK cells. All retained ability to activate MK DNA synthesis. Gain of activity mutants 7m10 and 7m11 with the substitutions in the G-box exhibited the least change from wild-type in the case of FGF-7. Mutants 7m5, 7m6, and 7m12 with alterations of short sequence domains on either side of the G-box with no gain of activity for 3T3 cells exhibited little change from wild-type activity.

Effect of C-terminal Alterations of FGF-7 and FGF-10 on Binding to Mammalian Cell Surface Receptors. To determine whether the gain of function conferred on FGF-7 and FGF-10 was reflected in the gain of binding to transmembrane FGFR embedded in the mammalian cell repertoire of pericellular matrix heparan sulfates, we tested the ability of the constructions to compete for binding of radiolabeled ^{125}I-FGF-1 which binds to all FGFR isoforms. The results confirmed that, parallel to the effects on

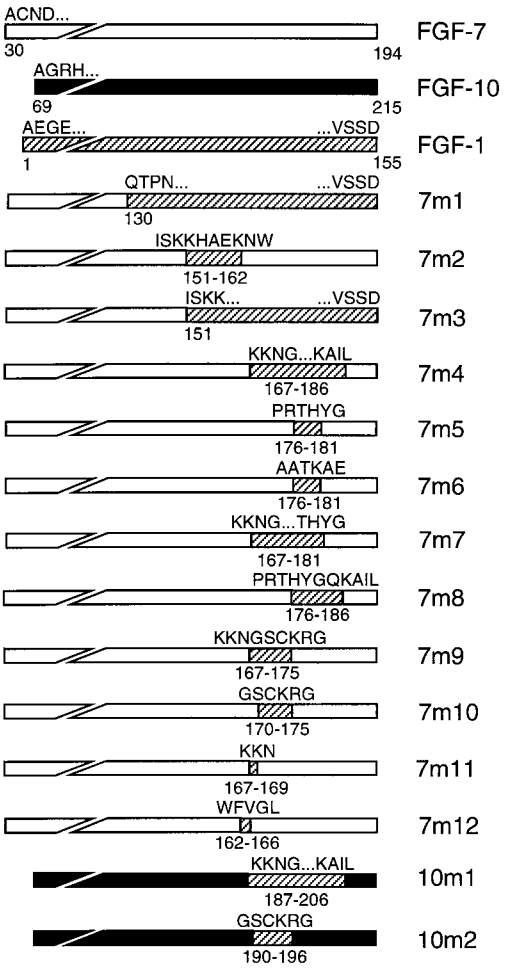

FIGURE 5: Schematic representation of recombinant constructions of FGF-7 and FGF-10. Sequences from FGF-7, FGF-10 and FGF-1 are shown by open, black, and hatched bars, respectively. In the mutant constructions, single-letter amino acid codes are from the FGF-1 sequence and the numbering is from the FGF-7 or FGF-10 sequence. Numbering is from the longest form of the three without the secretory signal sequence in the case of wild-type FGF-7 and FGF-10. 7m and 10m indicate mutants of the FGF-7 or FGF-10 backbone, respectively.

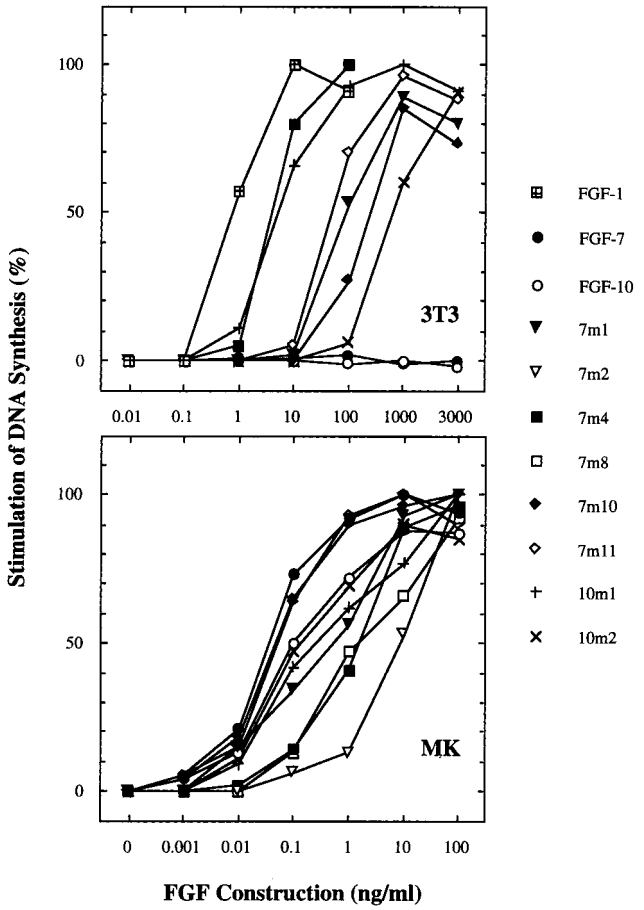

FIGURE 6: Effect of alterations in the C-terminal domain of FGF-7 and FGF-10 on mitogenic activity for mouse 3T3 fibroblasts and MK keratinocytes. The construction indicated on the right was added to cultures of quiescent 3T3 and MK cells maintained under conditions described in Materials and Methods. DNA synthesis was determined by thymidine incorporation. Activity is expressed as a percentage of the maximum level of thymidine incorporation stimulated by wild-type FGF-1 in 3T3 cells and FGF-7 in MK cells. The data points are the means of three independent experiments determined prior to conversion to a percentage. Maximum stimulation (100%) by FGF-1 of 3T3 cells was 28580 ± 2000 and 6477 ± 400 cpm for stimulation of MK cells by FGF-7.

mitogenesis, 7m1, 7m4, 7m10, 7m11, 10m1, and 10m2 gained ability to bind to receptors displayed on the 3T3 cells relative to the parent FGF-7 and FGF-10 with which competition was less than 10% at concentrations up to 10 μg/mL (Figure 7, Table 1). Mutants 7m10 and 7m11 with FGF-1 substitutions within the G-box supported gain of activity with the least change from wild-type. FGF-10 mutant constructs, 10m1 and 10m2, exhibited a much greater gain of mitogenic activity for 3T3 cells than was apparent in the competition binding assays (Table 1). Currently, this discrepancy is unexplained.

Effects of Substitutions in the C-terminus on Binding to Heparin. To determine whether alterations in the C-terminus of FGF altered the interaction with heparin, we immobilized constructs on heparin−agarose and eluted them with a gradient of increasing sodium chloride (Figure 8). Wild-type FGF-1 and FGF-10 elute from heparin at about 1.0−1.2 M NaCl while the affinity of FGF-7 is less with elution at 0.70−0.90 M. Gain-of-function mutants 7m1 and 10m1, in which sequences running to the end of the C-terminus were substituted with those of FGF-1, exhibited the largest increase in affinity for heparin. Mutants 7m4 and 7m6, one of which exhibiting a gain of function and the other displaying no change relative to wild-type, showed the largest decrease in affinity for heparin. Mutants, which exhibited no significant change in affinity for heparin, showed both gain and no gain of function on 3T3 cells. Some mutants in the latter class also exhibited no loss and some a significant loss in activity on MK cells. The results indicated no correlation between changes in affinity for heparin and changes in activity of the mutant constructions.

Effect of C-terminal Alterations of FGF-7 and FGF-10 on Binding to Recombinant FGFR Expressed in Insect Cells. To minimize the interference of mammalian cell pericellular matrix heparan sulfate, we examined the ability of mutants to compete with radiolabeled FGF-1 bound to recombinant FGFR1IIIc, FGFR2IIIb, and FGFR2IIIc at a high ratio of FGFR to endogenous matrix on the surface of baculoviral-infected insect cells. The results indicated that mutations, 7m1, 7m4, 7m10, and 7m11, which stimulated and bound to both 3T3 and MK cells, also competed with the binding of FGF-1 to both IIIc and IIIb isoforms of FGFR (Figure 9).

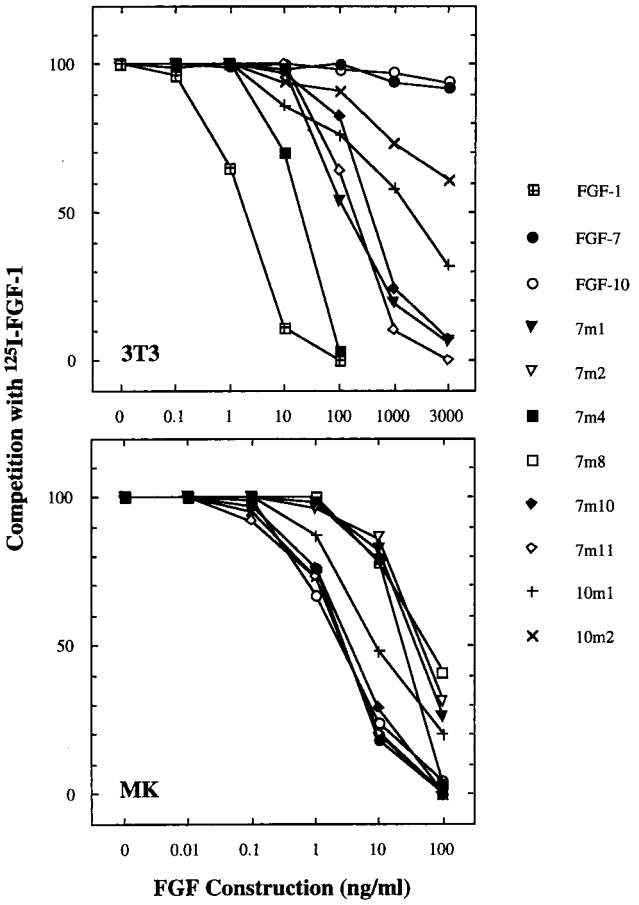

FIGURE 7: Binding to cell surface receptors of 3T3 fibroblasts and MK keratinocytes. The indicated concentrations of constructions were added to monolayers of cells in assay mixtures containing 2 ng/mL of native bovine ^{125}I-FGF-1. The specific data is representative of three separate experiments among which the variation was less than 10%. The mean of 100% binding from the three experiments was 1.5 ($\pm$ 0.11) $\times$ 10^4 cpm of bound FGF-1 in the absence of unlabeled FGF.

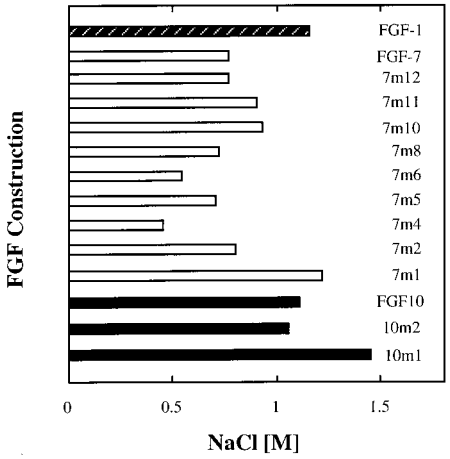

FIGURE 8: Effects of alterations in the C-terminus of FGF-7 and FGF-10 on affinity for heparin. The indicated FGF constructions were immobilized on heparin−agarose and then eluted by a linear gradient of sodium chloride from 0.15 to 2.15 M. The concentration of NaCl at the peak of elution monitored at A280 is indicated.

Finally, mutants 7m4 and 7m10 were radiolabeled and tested for covalent affinity cross-linking to FGFRIIIc to ensure that the gain of activity was a direct consequence of the gain in ability to dock into the ectodomain of FGFRIIIc

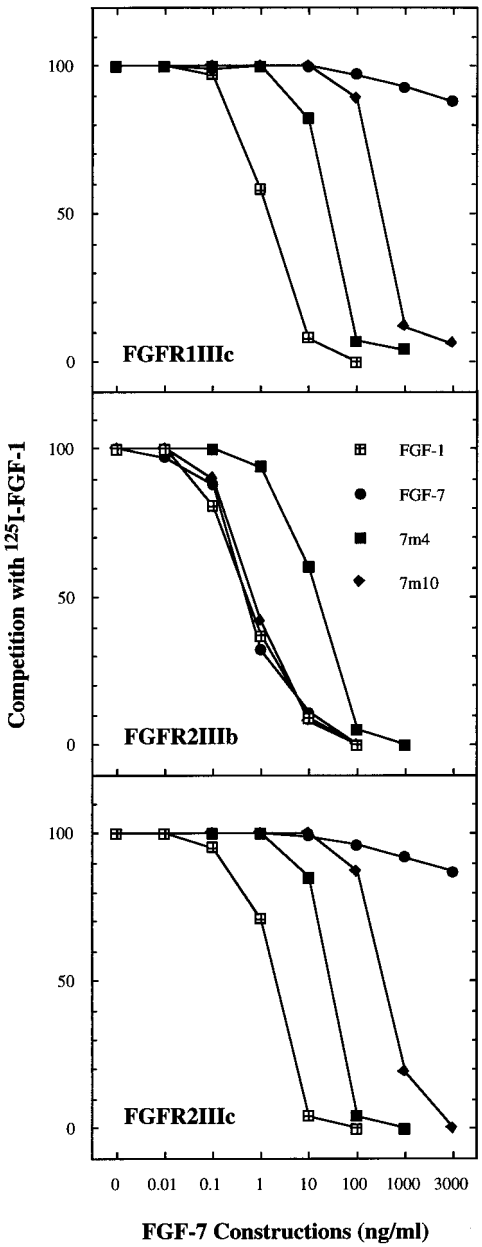

FIGURE 9: Binding of wild-type and mutant constructions to recombinant insect cell FGFR1IIIc, FGFR2IIIb, and FGFR2IIIc. The three FGFR isotypes were expressed on the surface of baculoviral-infected insect cells. The indicated amounts of unlabeled FGF constructs were added into binding assays containing 2 ng/mL of native bovine ^{125}I-FGF-1. Data were expressed as the percent of FGF-1 bound in absence of unlabeled FGF. The data shown represents one of three independent experiments. The mean of the 100% values among three experiments for each of the FGFR1IIIc, FGFR2IIIb, and FGFR2IIIc isoforms was 1.8 ($\pm$ 0.21), 2.5 ($\pm$ 0.18), and 1.2 ($\pm$ 0.15) $\times$ 10^4 cpm, respectively, which was representative of the variation among experimental points from the three trials.

in a conformation subject to covalent cross-linking. Radiolabeled mutant constructs both bound and cross-linked to all isoforms of FGFR1IIIc, FGFR2IIIb, and FGFR2IIIc (Figure 10).

DISCUSSION

The rejection of FGF-7 by isoforms of FGFR other than the specific splice variant FGFR2IIIb makes it the most specific among the ligands of the FGF family (*6*). Since

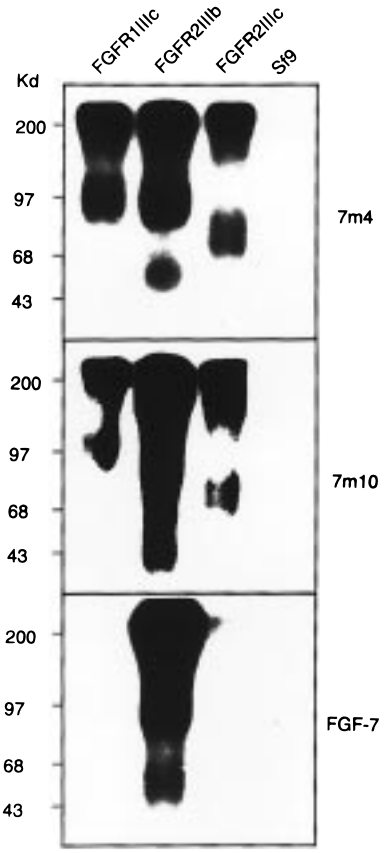

FIGURE 10: Covalent affinity cross-linking of radiolabeled gain-of-function chimeras of FGF-7−FGF-1. Wild-type FGF-7 and mutant constructs 7m4 and 7m10, respectively, were radiolabeled with ^{125}I, bound to baculoviral-infected Sf9 cells expressing the indicated FGFR, and cross-linked, and the radiolabeled complexes were analyzed by SDS−PAGE and autoradiography.

FGF-7 is generally expressed in mesenchymal or stromal cells within tissues with both epithelial and stromal compartments, and the expression of FGFR2IIIb is in the epithelial cells, it is the basis for a directionally specific signal from stroma to epithelium (*1, 7, 8*). In contrast, FGF-1 binds all isoforms of FGFR including FGFR2IIIb that have been analyzed to date (*1, 6*). Several studies using mutant constructions of FGF in diverse assay systems have suggested structural domains and specific residues that may be involved in the interaction of FGF with FGFR (*11, 12, 19, 26−28*). As a candidate structural cassette that might affect the specificity of FGF, a characteristic solvent-exposed loop that differs in the crystal structures of FGF-1 and FGF-2 has been focused on (*2−4*). By using mutagenesis, isothermal titration calorimetry, and molecular modeling, Springer et al. (*26*) found little impact of the loop domain, ^{110}KYTSW^{114}, on the binding of FGF-2 to FGFR but implicated the structure in mitogenesis induced by FGF. They proposed that the loop might be a low-affinity-binding site required for ligand stabilization of dimerization of FGFR. Seddon et al. (*12*) showed that substitution of the corresponding domain, ^{115}KKHAEKH^{121}, in FGF-1 and interleukin-1β (IL1β) increased affinity of FGF-2 for FGFR2IIIb. Reich-Slotky et al. (*13*) analyzed chimeric constructions comprising long stretches of FGF-7 and FGF-2 and concluded that the N-terminal portion of FGF-7, particularly residues 91−110, are the most important for the specificity for FGFR2IIIb. More recently, studies using molecular hybrids between zebrafish and Xenopus FGF-3, which bind FGFR2IIIb but differ in affinity for FGFR2IIIc, implicate the C-terminal portion in the specificity of the interaction with FGFR2IIIb (*9*).

In this study, we performed structure−function analysis employing the FGF-7 backbone to further pinpoint sequence domains involved in its failure to bind FGFRIIIc. At first, we experienced problems in expression and recovery of both wild-type and particularly mutants of FGF-7 in bacteria relative to FGF-1 and FGF-2. We devised an improved and novel method employing production of an inactive N-terminal fusion protein in the bacteria and subsequent proteolytic removal of the N-terminus and activation of the product while immobilized on heparin. The method facilitated production of diverse soluble mutant constructs of sufficient stability and purity to evaluate in mitogenic and radioreceptor binding assays. On the basis of corresponding sequence domains assigned in the crystal structure of FGF-1 and FGF-2 by Zhu et al. (ref *2*, Figure 4), substitution of the C-terminal sequence spanning the entire exon 3 beginning after β-strand 7 (β-strands 8−12 and intervening sequences), the sequence between β-strand 10 and 12, the 6-residue β-strand 11 sequence, or minimally the tripeptide sequence between β-strand 10 and 11 conferred ability to bind FGFRIIIc on FGF-7. We propose to call the 9-residue sequence comprised of the latter two sequences the "glycine or G-box" domain. In contrast, substitution of FGF-1 sequence domains on either side of the G-box, including the solvent-exposed loop between β-strands 9 and 10, failed to confer gain of activity on FGF-7 for FGFRIIIc. Substitution of the C-terminal domain of FGF-1 or part of the G-box sequence into FGF-10 also conferred a gain in ability to bind and activate FGFRIIIc. FGF-10 is a homologue of FGF-7 whose expression is limited to mesenchymal cells and binds FGFR2IIIb, but is rejected by FGFRIIIc. These results suggest that the G-box is a major determinant underlying the specificity of FGF-7. The structural domain may contribute to the specificity of other members of the FGF family for heparan sulfate−FGFR duplexes.

The experiments presented here were guided by previously described models of a ternary complex of the FGFR ectodomain, a single hexadecameric chain of heparin and FGF (*19, 25*). Models of the ternary complex of FGF-1 or FGF-2, FGFR1IIIc, and heparin indicated that the G-box is a focal point of the three-way interaction (Figure 3). Models in which FGF-7 was substituted for FGF-1 or FGF-2 revealed a spatial conflict between the G-box sequence domain and the fl1-C strand domain within Ig module III of FGFR1IIIc. The conflict is not present in a model of FGF-7 docked into the duplex of heparin and FGFR2IIIb. The experimental results presented here confirmed the predictions of the model that the conflict between FGF-7 and FGFRIIIc would be relieved by replacement of C-terminal sequences containing the G-box with the corresponding sequences from FGF-1. This is consistent with our previous report that removal by either trypsin or mutation of the C-terminal sequence of FGFR1IIIc beginning with the fl1 domain relieves the rejection of FGF-7 by the IIIc variant (*11*).

Analysis of the structure of FGF-2 by high-resolution NMR in solution revealed an α-helix-like structure formed by G-box residues ^{131}GQYKLG^{136} instead of the β-strand conformation (β-strand 11) predicted from the crystal structure (*18*). FGF-3, FGF-7, and FGF-10, all of which

are absolutely rejected by FGFRIIIc isoforms but bind FGFR2IIIb, exhibit a proline residue at position 6 of the G-box that may alter or disrupt the helical structure and, therefore, the fit into FGFRIIIc. The 9-residue G-box is conserved in all 17 of the currently identified FGF homologues with respect to length and in all, except FGF-15 and 17, with respect to presence and spacing of the two glycines (Figure 4). Except for FGF-15, basic residues at positions 2 and 7 or 8 of the G-box appear to be consensus residues. FGF-3, FGF-7, and FGF-10 that bind FGFR2IIIb, but are rejected by FGFRIIIc, are exceptions to the basic consensus residue at position 2 that is otherwise conserved in all 17 FGFs. Among the three, FGF-3 (*9*) and FGF-10, which bind FGFR1IIIb in addition to FGFR2IIIb (Lu, Luo, Kan, and McKeehan, manuscript in preparation), exhibit a glycine at position 2, while FGF-7, which uniquely binds only FGFR2IIIb, has a glutamine at that position. FGF-7 uniquely exhibits a hydrophobic valine residue at position 7, while FGF-3 and FGF-10 maintain the consensus basic residue (arginine). These combined unique features of the FGF-7 G-box may underlie its unique specificity. It should be noted, however, that the G-boxes of FGF-3 from xenopus and zebrafish, which are rejected by and bind FGFRIIIc, respectively, are identical (*9*). This suggests that the G-box is not a completely independent structural module, but cooperates with other sequence domains of FGF.

A heparin hexasaccharide contacts arginine and lysine residues at position 2 and 7 within the G-box of FGF-2 in cocrystals (*5*). In models of the ternary complex with FGF-1, FGF-2, FGF-7, and FGF-10, receptor-bound, fully sulfated heparin is in proximity to the G-box of each (ref *19*, Figure 3 and detail not shown here). Encounters between G-box residues of FGF-7 and heparin become more intimate in the model of the wild-type FGF-7−heparin−FGFRIIIc complex than FGF-1 and FGF-2 and the FGF-7−FGF-1 chimera, mFGF-7 (7m4). This suggests that interactions between the G-box and heparin might also contribute to rejection of FGF-7. However, we conclude that primarily determinants in the G-box and the ectodomain of the FGFRIIIc isoforms underlie rejection of FGF-7 rather than the composition of heparan sulfate. This is consistent with results that fail to demonstrate a correlation of changes in the interaction with heparin and the activity of the mutant constructions studied here. In addition, FGF-7 also fails to bind FGFRIIIc under artificial conditions devoid of heparin, whereas FGF-1 binding can be detected in the absence of heparin (ref *25* and unpublished results). We predict that cooperation between the heparan sulfate chain and the G-box may be a determinant of specificity when interaction with epitopes in the FGFR ectodomain is not the limiting factor.

ACKNOWLEDGMENT

We are grateful to Makiko Kan and Thanh T. Tran for their excellent technical assistance.

REFERENCES

1. McKeehan, W. L., Wang, F., and Kan, M. (1998) *Prog. Nucleic Acid Res. Mol. Biol. 5*, 135−176.
2. Zhu, X., Komiya, H., Chirino, A., Faham, A., Fox, G. M., Arakawa, T., Hsu, B. T., and Rees, D. C. (1991) *Science 251*, 90−93.
3. Eriksson, A. E., Cousens, L. S., Weaver, L. H., and Matthews, B. W. (1991) *Proc. Natl. Acad. Sci. U.S.A. 88*, 3441−3445.
4. Zhang, J., Cousens, L. S., Barr, P. J., and Sprang, S. R. (1991) *Proc. Natl. Acad. Sci. U.S.A. 88*, 3446−3450.
5. Faham, S., Hileman, R. E., Fromm, J. R., Linhardt, R. J., and Rees, D. C. (1996) *Science 271*, 1116−1120.
6. Ornitz, D. M., Xu, J., Colvin, J. S., McEwen, D. G., MacArthur, C. A., Coulier, F., Gao, G., and Goldfarb, M. (1996) *J. Biol. Chem. 271*, 15292−15297.
7. Yan, G., Yoshitatsu, F., Nikolaropoulos, S., Wang, F., and McKeehan, W. L. (1992) *Mol. Endocrinol. 12*, 2123−2128.
8. Yan, G., Fukabori, Y., McBride, G., Nikolaropoulos, S., and McKeehan, W. L. (1993) *Mol. Cell. Biol. 13*, 4513−4522.
9. Kiefer, P., Mathieu, M., Mason, I., and Dickson, C. (1996) *Oncogene 12*, 1503−1511.
10. Beer, H. D., Florence, C., Dammeier, J., McGuire, L., Werner, S., and Duan, D. R. (1997) *Oncogene 15*, 2211−2218.
11. Wang, F., Kan, M., Xu, J., Yan, G., and McKeehan, W. L. (1995) *J. Biol. Chem. 270*, 10222−10230.
12. Seddon, A. P., Aviezer, D., Li, L.-Y., Böhlen, P., and Yayon, A. (1995) *Biochemistry 34*, 731−736.
13. Reich-Slotky, R., Shaoul, E., Berman, B., Graziani, G., and Ron, D. (1995) *J. Biol. Chem. 271*, 29813−29818.
14. Baird, A., Schubert, D., Ling, N., and Guillemin, R. (1988) *Proc. Natl. Acad. Sci. U.S.A. 85*, 2324−2328.
15. Yayon, A., Aviezer, D., Safran, M., Gross, J. L., Heldman, Y., Cabilly, S., Givol, D., and Katchalski-Katzir, E. (1993) *Proc. Natl. Acad. Sci. U.S.A. 90*, 10643−10647.
16. Wong, P., Hampton, B., Szylobryt, E., Gallagher, A. M., Jaye, M., and Burgess, W. H. (1995) *J. Biol. Chem. 270*, 25805−25811.
17. Wang, F., Kan, M., McKeehan, K., Jang, J.-H., Feng, S., and McKeehan, W. L. (1997) *J. Biol. Chem. 272*, 23887−23895.
18. Moy, F. J., Seddon, A. P., Böhlen, P., and Powers, R. (1996) *Biochemistry 35*, 13552−13561.
19. Luo, Y., Gabriel, J. L., Wang, F., Zhan, X., Maciag, T., Kan, M., and McKeehan, W. L. (1996) *J. Biol. Chem. 271*, 26876−26883.
20. Kan, M., Shi., E., and McKeehan, W. L. (1991) *Methods Enzymol. 198*, 158−171.
21. McKeehan, W. L., Wu, X., Jang, J., and Kan, M. (1997) *In Vitro Cell. Dev. Biol. 33*, 727−730.
22. Ron, D., Bottaro, D. P., Finch, P. W., Morris, D., Rubin, J. S., and Aaronson, S. A. (1992) *J. Biol. Chem. 268*, 2984−2988.
23. Nybo, R. E., Everton, E. N., and Morris, C. F. (1997) *In Vitro Cell. Dev. Biol.: Anim. 33*, 606−607.
24. Hsu, Y.-R., Hsu, E. W−J., Katta, V., Brankow, D., Tseng, J., Hu, S., Morris, C. F., Kenney, W. C., and Lu, H. S. (1998) *Protein Expression Purif. 12*, 189−200.
25. Kan, M., Wang, F., Kan, M., To, B., Gabriel, J. L., and McKeehan, W. L. (1996) *J. Biol. Chem. 271*, 26143−26148.
26. Springer, B. A., Pantoliano, M. W., Barbera, F. A., Gunyuzlu, P. L., Thompson, L. D., Herblin, W. F., Rosenfeld, S. A., and Book, G. W. (1994) *J. Biol. Chem. 28*, 26879−26884.
27. Zhu, H., Ramnarayan, K., Anchin, J., Miao, W. Y., Sereno, A., Millman, L., Zheng, J., Balaji, V. N., and Wolff, M. E. (1995) *J. Biol. Chem. 37*, 21869−21874.
28. Zhu, H., Anchin, J., Ramnarayan, K., Zheng, J., Kawai, T., Mong, S., and Wolff, M. E. (1997) *Protein Eng. 10*, 417−421.

BI9816599